**Atmospheric
Chemistry
and Physics
Discussions**

ACE-FTS measurements of trace species in the characterization of biomass burning plumes

K. A. Tereszchuk[1], G. González Abad[1], C. Clerbaux[2,3], D. Hurtmans[3], P.-F. Coheur[3], and P. F. Bernath[1]

[1]Department of Chemistry, University of York, Heslington, York, YO10 5DD, UK
[2]UPMC Univ. Paris 06, Université Versailles St-Quentin, CNRS/INSU, LATMOS-IPSL, Paris, France
[3]Spectroscopie de l'Atmosphère, Service de Chimie Quantique et de Photophysique, Université Libre de Bruxelles (U.L.B.), Brussels, Belgium

ACPD

11, 16611–16637, 2011

**ACE-FTS
measurements of
trace species**

K. A. Tereszchuk et al.

Full Screen / Esc

Printer-friendly Version

Interactive Discussion

Abstract

To further our understanding of the effects of biomass burning emission on atmospheric composition, we report measurements of trace species from biomass burning plumes made by the Atmospheric Chemistry Experiment Fourier Transform Spectrometer (ACE-FTS) instrument on the SCISAT-1 satellite. An extensive set of 15 molecules, C_2H_2, C_2H_6, CH_3OH, CH_4, CO, H_2CO, HCN, HCOOH, HNO_3, NO, NO_2, N_2O_5, O_3, OCS and SF_6 are used in our analysis. Even though most biomass burning smoke is typically confined to the boundary layer, much of these emissions are injected directly into the free troposphere via fire-related convective processes and transported away from the emission region. Further knowledge of the aging of biomass burning emission in the free troposphere is needed. Tracer-tracer correlations are made between known pyrogenic species in these plumes in an effort to classify them and follow their chemical evolution. Criteria such as age and type of biomass material burned are considered. Emission factors are derived and compared to airborne measurements of biomass burning from numerous ecosystems to validate the ACE-FTS data.

1 Introduction

Biomass burning has an important role in determining the composition of the Earth's surface and atmosphere, and in some regions emissions to the atmosphere rival those from fossil fuel combustion. For nearly 40 years the scientific community has studied the emission of trace constituents from different types of fuel and associated atmospheric concentrations, but our knowledge remains incomplete, reflecting the heterogeneous and stochastic nature of this process. The advent of space-borne observations of land-surface and tropospheric composition provided the first glimpse of the large-scale impact of burning in the global troposphere, where biomass burning events represent an important source of gases and particles released into the atmosphere (Crutzen et al., 1979; Crutzen and Andreae, 1990; Andreae and Merlet, 2001).

Title Page

Abstract | Introduction

Conclusions | References

Tables | Figures

◀ | ▶

◀ | ▶

Back | Close

Full Screen / Esc

Printer-friendly Version

Interactive Discussion

Wildfires significantly alter air quality, sometimes on regional to hemispheric scales, and are an important component of the climate system. Biomass burning is, indeed, now recognized to be a major contributor to the global emissions of chemically-active trace gases and aerosols. A wide variety of pyrogenic species are emitted, including carbon dioxide (CO_2), carbon monoxide (CO), methane (CH_4) plus a series of volatile organic hydrocarbons (VOCs), oxygenated volatile organic compounds (OVOCs) as well as nitrogen-, sulfur- and halogen-containing species, which are transformed by photochemical processes occurring during the first few hours in the plume. These molecules significantly alter the distribution of tropospheric ozone (O_3) and affect the oxidizing capacity of the atmosphere (Coheur et al., 2007).

The immediate goal of this work is to report and interpret the tropospheric mixing ratios of short- and long-lived trace molecular species from biomass burning emission obtained from infrared solar occultation measurements made with the Atmospheric Chemistry Experiment Fourier Transform Spectrometer (ACE-FTS) instrument on the SCISAT-1 satellite (Bernath et al., 2005). Tracer-tracer correlation calculations are carried out between known pyrogenic species in an attempt to differentiate and characterize biomass burning emission both temporally as plumes evolve over time and qualitatively by comparing mixing ratios associated with different fuel types.

This preliminary work is part of an in-depth and more rigorous study being carried out in order to characterize biomass burning plumes remotely by considering criteria such as age and type of biomass material, and will be an integral facet of the Quantifying the impact of BOReal forest fires on Tropospheric oxidants over the Atlantic using Aircraft and Satellites (BORTAS) project (http://www.geos.ed.ac.uk/research/eochem/bortas/) to further our understanding of the impact of biomass burning on atmospheric chemistry. Included in this study will potentially be the addition of new VOC and OVOC species including acetonitrile (Allen et al., 2011) and acetaldehyde (Tereszchuk et al., 2011) to be retrieved by ACE-FTS to aid in plume differentiation and characterization. Additional goals of this study will be to validate aircraft measurements made during the BORTAS flight campaign and to derive age-dependent emission ratios (Andreae and

Merlet, 2001) which will serve as constraints for atmospheric models.

ACE-FTS is a high-resolution Fourier transform spectrometer used for remote sensing of the limb of the Earth's atmosphere down to 5 km. ACE-FTS has wide spectral coverage in the infrared covering a continuous region from 750 to 4400 cm^{-1} and currently offers, through the recently released Version 3.0 dataset (http://www.ace.uwaterloo.ca), retrievals for 38 molecular species as well as their isotopologues, over a dozen of which are known primary pyrogenic species found in biomass burning. With this large suite of molecular species available and near global coverage, the ACE-FTS is currently the most suitable remote-sensing instrument for this type of detailed investigation.

Previous studies of biomass burning emissions have been performed using ACE-FTS (Rinsland et al., 2005, 2007; Coheur et al., 2007) as well as a variety of other space-borne instruments (Turquety et al., 2009; Coheur et al., 2009; Glatthor et al., 2009; Torres et al., 2010). The initial work conducted using ACE-FTS studied the emission of longer-lived primary pyrogenic species and their long-range transport to establish the effectiveness of ACE-FTS in measuring the emission of trace species from biomass burning (Rinsland et al., 2005). This work was followed up by a more extensive analysis of the elevated volume mixing ratios for numerous species emitted from young Boreal plumes, deriving emission factors and calculating tracer-tracer correlation coefficients to demonstrate their enhancement (Rinsland et al., 2007). Results from these works sparked interest in retrieving additional trace organic species from biomass burning such as ethene (C_2H_4), propyne (C_3H_4), formaldehyde (H_2CO), acetone (C_3H_6O) and peroxyacetylnitrate, abbreviated as PAN ($CH_3COO_2NO_2$), and were the first reported detections of these species using infrared solar occultation spectroscopy from satellites (Coheur et al., 2007).

Biomass burning releases primary pyrogenic gases and primary smoke particles whose characteristics and relative emissions depend on various factors including the particular type of material burned and the burning conditions, e.g. flaming or smoldering combustion (Koppmann et al., 2005). This has been demonstrated by Yokelson et

Full Screen / Esc

Printer-friendly Version

Interactive Discussion

al. (1997), where biomass samples from a variety of ecosystems were burned at the Intermountain Fire Sciences Laboratory in Missoula, Montana. Yokelson et al. (1997) measured the emission from the smoldering combustion of biomass with a Fourier transform infrared spectrometer (FT-IR) coupled to an open multipass cell. Numerous, highly successful, field campaigns have also been conducted in an effort to quantify and characterize emissions from biomass burning from different ecosystems such as the the work done by Yokelson et al. (2003) to study the emissions from nascent and aged plumes from the African savannah and the forests of Amazonia in Brazil during the TROFFEE campaign during the 2004 dry season (Yokelson et al., 2007b); but given the highly variable emissions inherent to biomass burning, even from within a single fire type (Akagi et al., 2010), it is uncertain whether this type of detailed characterization can be carried out with space-borne measurements and has yet to be confirmed.

2 Methodology

2.1 Plume identification

In previous studies conducted with ACE-FTS on the identification of biomass burning plumes, carbon monoxide (CO) was the principal molecular species used to find occultations that sample biomass burning plumes through enhanced concentrations of CO relative to the background. CO is a well-known pyrogenic species with an atmospheric lifetime of ∼2 months in the free troposphere. Because CO is also emitted from numerous anthropogenic sources, another long-lived species that is more specific to biomass burning was chosen for our work. Hydrogen cyanide (HCN) has a life time of ∼5 months and is emitted almost entirely from biomass and biofuel combustion. Typical background concentrations for HCN in the free troposphere have been determined to be 0.225–0.250 ppb (Li et al., 2003; Singh et al., 2003). In our work, occultations with enhanced tropospheric concentrations of HCN ≥0.350 ppb were considered as measurements of biomass burning emission.

Full Screen / Esc

Printer-friendly Version

Interactive Discussion

2.2 ACE-FTS data processing

To isolate retrievals made in the free troposphere, values for tropopause heights were obtained from derived meteorological products (DMPs) that were created using the ACE-FTS Version 3.0 dataset (Manney et al., 2007); all measurements above the altitude corresponding to the tropopause were filtered out. Data obtained from below the tropopause was then filtered by calculating the median values of each of the molecular species to be studied. Retrievals which contained measurements with values that were less than 10 % of the median value were rejected as this usually indicates a failure in the retrieval. The remainder of this data was then filtered by calculating the median absolute deviation (MAD) of the associated measurement errors; if the measurement error was greater than 100 times the MAD value calculated from the dataset, they too were rejected. With the data thus filtered for any erroneous measurements, those occultations which contained HCN altitude profiles with concentrations of HCN ≥0.350 ppb were deemed measurements of biomass burning plumes and measurements with concentrations of HCN ≤0.260 ppb treated as background measurements.

2.3 Plume source location

Once plume measurements from the ACE-FTS dataset were identified, the biomass burning source location that corresponds to a particular occultation was determined. To do this, fire data obtained from algorithm 1 of the night time data from the Advanced Along Track Scanning Radiometer (AATSR) World Fire Atlas (Arino and Plummer, 2001) was used concertedly with the HYbrid Single-Particle Lagrangian Integrated Trajectory (HYSPLIT) (Draxler and Rolph, 2003) model. The altitudes corresponding to the maximum value for the concentration of HCN in the ACE-FTS retrieval profiles were used as the starting point in HYSPLIT to calculate back trajectories of the air mass from the point of measurement to recorded instances of biomass burning. In this way, the relative age of the plume can be determined with an accuracy of ±1 day. An example of plume identification from calculated back trajectories made with HYSPLIT is seen

Title Page

Abstract | Introduction

Conclusions | References

Tables | Figures

◄ | ►

◄ | ►

Back | Close

Full Screen / Esc

Printer-friendly Version

Interactive Discussion

in Fig. 1, where the outflow from Boreal fires burning in northern Saskatchewan and parts of the Northwest Territories in Canada (29 July 2010) are measured over Maritime Canada 3 days later by ACE-FTS (sunset occultation ss37484). To validate the AATSR fire data, MODIS Terra and Aqua fire products were also utilized to verify the location of biomass burning. Given that the MODIS data provided by the University of Maryland (ftp://fuoco.geog.umd.edu) is for 8-day and monthly fire activity, the AATSR data was preferentially used where fire hot spots have information on the specific date of measurement, providing better temporal resolution to determine the location of instances of biomass burning.

A visualization tool was required to bring ACE occultations, the AATSR and MODIS fire data and HYSPLIT trajectories together in order to facilitate the determination of plume origins. Scripts were written in Keyhole Markup Language (KML) in order to import the locations of ACE occultations and instances of fire activity into Google™Earth along with the air mass trajectories. HYSPLIT conveniently provides the option for output into the KML format. An additional benefit of using Google™Earth is that once instances of biomass burning are geographically determined, one can visually inspected the region to help verify the biomass material that is being burned. For example, a fire in the Amazon could be a deforestation fire, an understory fire, a crop residue fire on a plantation, or a pasture fire. Google™Earth along with the use of the Near-Real-Time Level-2 Data from the MODIS Rapid Response System (http://rapidfire.sci.gsfc.nasa.gov/realtime/?calendar) can assist in elucidating what material is actually contributing to the biomass emission.

To further assist in the verification of the origin of biomass burning plumes, CO total column measurements from the Infrared Atmospheric Sounding Interferometer (IASI) on board the MetOp-A satellite (George et al., 2009; Clerbaux et al., 2009) were used to visualize the outflow of biomass burning sources to ensure that measurements are from a singular origin and not a mixture of biomass burning outflows from different locations, which would compromise plume characterization. For example, plumes measured over the North Atlantic can come from a number of different geographical locations since it is

a region that corresponds to the confluence of numerous air masses. During the summer in the northern hemisphere, fire activity is prevalent in Canada, Alaska, Siberia and California. Simultaneous outflows from each of these regions will often converge over Eastern Canada and the North Atlantic, creating uncertainty in the analysis of plume origin and age. Figure 2 shows an example of IASI CO total column measurements made over Canada on 29 July 2010. In it, biomass burning plumes can be clearly seen over Canada from fires in northern Saskatchewan and the Northwest Territories, a Siberian plume making its way eastward over Arctic Canada and a plume originating from eastern China is drifting towards the west coast of North America.

2.4 Tracer-tracer correlations

Tracer-tracer correlation studies were conducted using 15 different molecular species. The majority of these species such as, C_2H_2, C_2H_6, CH_3OH, CH_4, CO, H_2CO, HCN, HCOOH, HNO_3 and OCS, are known primary pyrogenic biomass burning species and have been previously studied with ACE-FTS. In addition to these, NO, NO_2, N_2O_5 and O_3 are investigated to observe the effect of biomass burning emission on tropospheric oxidants. Finally, SF_6 was also included in the study. Although it was demonstrated by Rinsland et al. (2007) that SF_6 does not correlate with the VMRs of species emitted from fires and that the SF_6 mixing ratio is consistent with no significant SF_6 emissions from biomass burning, we treat SF_6 in this work as a reference species to identify any potentially anomalous results in our calculations.

Further data filtering was conducted during the correlation calculations where only the altitudes with values of HCN ≥ 0.35 ppb were used. Figure 3 is an example of a tracer-tracer correlation of ethane (C_2H_6) and CO for a young (2-3 day old) Boreal biomass burning plumes from July 2008. C_2H_6 is a known primary pyrogenic species emitted from biomass burning and the upper panel of Fig. 3 verifies its presence as it correlates highly with CO in plumes ($R = 0.931$) and poorly in the background measurements ($R = 0.512$) seen in the lower panel.

3 Results

3.1 Plume characterization

ACE-FTS measurements for the months of July and October from 2004 to 2010 were analyzed in an effort to characterize biomass burning from different ecosystems found in both the northern and southern hemisphere. The month of October falls within the burning season in the Amazon of South America and the Congo in Africa, where slash-and-burn agriculture is prevalent. This month also coincides with a period of typically high fire activity in the Australian savannah. July is at the height of forest fire activity in Canada, Alaska, California and Russia, as well as parts the Mediterranean basin, particularly in Spain and Greece.

Table 1 gives a summary of R coefficients from tracer-CO correlations calculated for sets of approximately 30 measurements of young biomass burning plumes, determined to be 2–3 days old, from the Amazon rainforest in Brazil, the jungle of the African Congo, the savannah grasslands of northern Australia and Boreal forests in Canada, respectively. As a reference, off-plume background calculations were conducted using ACE-FTS measurements at similar latitudes during the same corresponding time periods. Beneath each R-value is the slope of the linear regression i.e. emission ratio with respect to CO (Andreae and Merlet, 2001), and the standard deviation associated with the calculation (shown in parentheses). The standard deviation was calculated assuming that the linear regression is expressed as:

$$Y_i = A + BX_i \tag{1}$$

then the standard deviation is evaluated as:

$$SD = \sqrt{\frac{\sum_{i=1}^{N}(y_i - (A + BX_i))^2}{N - 2}} \tag{2}$$

Highlighted in each ecosystem are those trace species which correlate highly with CO ($R \geq 0.80$). Upon inspection, it is apparent that the biomass emissions from each of

the four examples provided possess a distinct composition of trace gases such that they may be characterized individually. For example, biomass burning emission from Congo shows a very high correlation for formaldehyde (H_2CO), but the Amazon and Australian savannah do not. Plumes from the Amazon and Australian savannah can be distinguished from one another due to the high negative correlation that Australian plumes possess for nitric acid (HNO_3).

It is known that as biomass burning plumes age, the emitted gaseous pyrogenic species within it react and chemical transformations of these primary pyrogenic species takes place leading to the formation of secondary species. Of these secondary species, O_3 and HNO_3 are particularly important. HNO_3 is formed by OH-induced conversion of NO_2, which results from rapid conversion of primary pyrogenic NO. NO_2 is also an important precursor to PAN which forms within a few hours of the source. At low temperatures in the free troposphere and in the presence of co-emitted NH_3, HNO_3 will quickly convert to ammonium nitrate (NH_4NO_3) (Yokelson et al., 2009; Alvarado et al., 2010). Organics emitted from biomass burning leads to the formation of secondary O_3, an important atmospheric oxidant, and a precursor of OH radicals (Fiedler et al., 2009; Akagi et al., 2010). It is well known that reactions with the hydroxyl radical (OH), the dominant oxidizing chemical in the atmosphere, drive atmospheric oxidation through reaction with chemicals emitted from the Earth's surface, thus creating new species that are more easily scavenged and removed by aerosols, clouds and rain. Many of these molecules lead to the chemical production of tropospheric O_3 and other reactive trace gases (Rinsland et al., 2005).

Although the data in this work is preliminary and a more extensive analysis of the entire ACE-FTS dataset will be required before any specific chemical properties of biomass burning emissions can be thoroughly justified, we can see from the correlations analysis for Boreal biomass burning in Canada and the savannah in northern Australia that, in addition to a high negative correlation for O_3, significant negative correlations for nitrogen dioxide (NO_2) and nitric acid (HNO_3) are also evident and strongly suggest that NO_2 and HNO_3 are also secondary species being created from Boreal

Back   Close

Full Screen / Esc

Printer-friendly Version

Interactive Discussion

forest and savannah grassland fire emissions that are 2–3 days in age.

Typically, negative correlations are taken as evidence of destruction not production; a negative value simply means that as one trace species increases in concentration the other species decreases. However, should the VMRs of O_3, HNO_3 and NO_2 increase
5 as the plume ages, this indicates a formation as a secondary species such that the primary pyrogenic species are reacting with the surrounding to form these secondary products. To confirm the observations, Table 2 lists the ratios that show the excess value above background normalized to excess CO above background, i.e. $\Delta X/\Delta CO$ where ΔX indicates the value of $X_{plume} - X_{background}$ for numerous trace species emitted
10 from Boreal biomass burning. Values are compared between plumes 1–2 days old and those that are 5–6 days old. As would be expected, the ratios for the primary pyrogenic species relative to long-lived CO decrease over time as these species are destroyed mainly by reaction with OH as the plume ages over time, but for O_3, NO_2, HNO_3, the negative correlations with a marked increased value for $\Delta X/\Delta CO$ occurs to support
15 the results of the tracer-CO correlations for Boreal fires in Table 1. This indicates that primary species emitted from Boreal fires are reacting with the surrounding atmosphere to produce O_3, NO_2 and HNO_3 as secondary pyrogenic species. Negative correlations are thus obtained for these secondary species because their concentration increases as concentrations for the primary pyrogenic species are decreasing.

20 As biomass burning emissions age over time, the composition of the plume will change as chemical processes create or destroy a particular trace gas. The formation of O_3 as a secondary species is a prime example as fresh Boreal biomass burning plumes contain no appreciable enhancement of O_3, as was demonstrated in the results ARCTAS-B campaign (Alvarado et al., 2010), but enhancements are clearly apparent
25 in the aged Boreal plumes measured in this work. NO_2 is a species that exhibits high variability in biomass burning emissions, as was also noted in the results of ARCTAS-B. The results from Table 1 show high negative correlations for NO_2 in 2–3 day old emissions from the Boreal and savannah fires, but a high positive correlation in emissions from the Amazon, indicating the possibility of NO_2 as both a primary and secondary

ACE-FTS measurements of trace species

K. A. Tereszchuk et al.

Full Screen / Esc

Printer-friendly Version

Interactive Discussion

pyrogenic species. Typically NO_2 emitted from biomass combustion is photolyzed to produce O_3 and combines with OH to create HNO_3, but the increase in concentration seen in the Boreal plumes that are 5–6 days old indicates a production process. Again, further analysis will need to be carried out to confirm the preliminary results obtained in this work.

Further exploring the capabilities of ACE-FTS to study the chemical evolution of biomass burning plumes, Fig. 4 shows an example of sequential measurements of a plume originating from the Amazon on 20 October 2004 that continuously flowed from the source over a period of several days. On 29 October 2004, 5 measurements were made in succession, 90 min between each measurement, sampling along the plume towards the source. The first measurement made was sr6528 where the age of the plume was some 8 days, each successive measurement corresponds to a difference in age of approximately a day and the final measurement, sr6532, sampled the outflow when it was approximately 4 days old. Table 3 lists the tracer-CO correlation coefficients for each of the occultations and the mean concentrations (in ppb) of each of the trace species measured.

It is apparent from the concentrations in Table 3 that many of the known pyrogenic species emitted from biomass burning have elevated values which diminish over time as the plume ages and the outflow disperses eastwards. Understandably there is some fluctuation in concentration from measurement to measurement due to the fact that in each instance the measurement made may not have been at the exact center of the plume, but the overall trend is evident. Even from correlations calculated from the few data points obtained from the individual occultations, these molecules correlate with CO with high positive values indicating their presence as primary pyrogenic species. Once again, reactions of the primary organic species lead to the formation of O_3, which shows a positive trend where concentrations of O_3 increase with age. Progressively larger negative values for the correlation coefficients confirm the results for Amazon plumes seen in Table 1, where O_3 is being generated as a secondary pyrogenic species from biomass burning emission and increases over time as the plume

ages. It is interesting to note that in the case of plumes originating from Amazonia, high positive correlations for NO_2 are obtained, indicating that it is being produced as a primary pyrogenic species unlike the biomass burning emissions from Boreal forests and savannah grasslands of the same age where NO_2 is produced as a secondary species. Occultation sr6529, one of the five successive measurements listed in Table 3, NO_2 correlates highly with CO ($R = 0.984$), which corresponds to the results observed from the correlations of young Amazon plumes in Table 1 where a value of $R = 0.971$ was obtained.

3.2 Emission factors

One of the goals of this study is to calculate sets of age-dependent emission ratios for biomass burning emission obtained from remote measurements of biomass burning plumes that can serve as constraints for atmospheric models in an effort to analyze plume aging and evolution.

To validate the emission ratios obtained from the preliminary results from this study, emission factors were derived for 5 primary pyrogenic species relative to CO using the emission ratios calculated for the young plumes listed in Table 1. The conventional approach was used for determining emission ratios and emission factors (Andreae and Merlet, 2001). Measured concentrations for each species were first plotted versus the corresponding concentration for CO (i.e. tracer-CO correlation). The slope of the linear regression is the associated emission ratio. The ACE-FTS data was converted from emission ratios with respect to CO to emission factors assuming the relation:

$$EF_X = ER_{(X/CO)} \cdot (MW_X / MW_{CO}) \cdot EF_{CO} \tag{3}$$

where EF_X is the emission factor for the molecular species X, $ER_{(X/CO)}$ is the molar emission ratio of the molecular species with respect to CO, MW_{CO} is the molecular weight of CO, and EF_{CO} is the emission factor of CO (Andreae and Merlet, 2001).

Table 4 lists the emission factors with respect to CO for C_2H_6, CH_3OH, HCN, HCOOH and OCS for the Boreal forests in Canada, the Amazon Rainforest and the savannah of

Full Screen / Esc

Printer-friendly Version

Interactive Discussion

northern Australia. We assumed CO emission factors of 126(45) g kg^{-1}, 92(26) g kg^{-1} and 59(16) g kg^{-1}, respectively for CO for dry matter, which were the estimated values for biomass burning determined for Boreal forests, tropical forests and savannah grasslands respectively from the extensive study conducted by Akagi et al. (2010). The

5 calculated emission factors for the 5 trace species were then compared to the values obtained by Akagi et al. (2010). In addition, the Boreal emission factors were also contrasted to previously made calculations from ACE-FTS measurements of boreal fires in Alaska and Canada for these same 5 trace species (Rinsland et al., 2007). The errors calculated for the emission factors take into account that the recommended values

10 obtained from Akagi et al. (2010) are themselves typically about 30 % uncertain at the 1-sigma level and are propagated through the calculation.

Upon inspection, we see that the calculated values for the emission factors from this study are in good agreement to those derived from the airborne measurements used in the work by Akagi et al. (2010) and fall well within the limits of the associated errors.

15 The only exceptions are for the emission factors of HCN and OCS associated with Boreal fires, where our values are an order of magnitude smaller than those reported by Akagi et al. (2010); although when compared to the emission factor obtained by Rinsland et al. (2007), our values confirm the emission factors of HCN and OCS previously obtained using ACE-FTS. Rinsland et al. (2007) also made note of this same

20 discrepancy when comparing their emission factors to the results obtained from the airborne measurements conducted by Yokelson et al. (1997). Given the few number of ACE-FTS measurements and that emission factors are being calculated using emission ratios from plumes 2–3 days old and not from fresh biomass burning emissions from which the emission factors provide by Akagi et al. (2010) are derived, the discrep-

25 ancy here is not totally unexpected.

4   Conclusions

Measurements of trace species from biomass burning plumes were made using the Atmospheric Chemistry Experiment Fourier Transform Spectrometer (ACE-FTS) instrument. An extensive set of molecules, C_2H_2, C_2H_6, CH_3OH, CH_4, CO, H_2CO, HCN, HCOOH, HNO_3, NO, NO_2, N_2O_5, O_3, OCS and SF_6 were used in our analysis. Tracer-tracer correlations were made between known pyrogenic species in these plumes in order to classify them and to follow their chemical evolution. The preliminary results of this investigation indicate that space-borne measurements of biomass burning emissions from different ecosystems can be characterized by their unique chemical composition and that the formation of secondary pyrogenic species can be effectively monitored.

Given the good agreement of the airborne emission factors with the remote-sensing data obtained from ACE-FTS measurements of biomass burning, we are confident that sets of age-dependent emission ratios for a variety of biomass burning sources can be derived using the ACE-FTS dataset, which can serve as constraints for atmospheric models and to assess the overall impact of biomass burning on atmospheric chemistry.

References

Akagi, S. K., Yokelson, R. J., Wiedinmyer, C., Alvarado, M. J., Reid, J. S., Karl, T., Crounse, J. D., and Wennberg, P. O.: Emission factors for open and domestic biomass burning for use in atmospheric models, Atmos. Chem. Phys., 11, 4039–4072, doi:10.5194/acp-11-4039-2011, 2011. 16615, 16620, 16624, 16633

Allen, N. D. C., Harrison, J. J., and Bernath, P. F.: Acetonitrile (CH_3CN) infrared absorption cross sections in the 3 µm region, J. Quant. Spectrosc. Ra., submitted, 2011. 16613

Alvarado, M. J., Logan, J. A., Mao, J., Apel, E., Riemer, D., Blake, D., Cohen, R. C., Min, K.-E., Perring, A. E., Browne, E. C., Wooldridge, P. J., Diskin, G. S., Sachse, G. W., Fuelberg, H., Sessions, W. R., Harrigan, D. L., Huey, G., Liao, J., Case-Hanks, A., Jimenez, J. L., Cubison, M. J., Vay, S. A., Weinheimer, A. J., Knapp, D. J., Montzka, D. D., Flocke, F. M., Pollack, I. B., Wennberg, P. O., Kurten, A., Crounse, J., Clair, J. M. St., Wisthaler, A., Mikoviny, T., Yantosca, R. M., Carouge, C. C., and Le Sager, P.: Nitrogen oxides and PAN in plumes from boreal fires during ARCTAS-B and their impact on ozone: an integrated analysis of aircraft and satellite observations, Atmos. Chem. Phys., 10, 9739–9760, doi:10.5194/acp-10-9739-2010, 2010. 16620, 16621

Andreae, M. O. and Merlet, P.: Emission of trace gases and aerosols from biomass burning, Global Biogeochem. Cy., 15, 955–966, doi:910.1029/2000GB001382, 2001. 16612, 16613, 16619, 16623

Arino, O. and Plummer, S.: Along Track Scanning Radiometer World Fire Atlas: Validation of the 1997–1998 Active Fire Product, Validation report, IGBP-DIS Working Pap. 23, Int. Geosph. Biosph. Progr., Stockholm, 2001. 16616

Bernath, P. F. McElroy, C. T., Abrams, M. C., Boone, C. D., Butler, M., Camy-Peyret, C., Carleer, M., Clerbaux, C., Coheur, P.-F., Colin, R., DeCola, P., DeMaziére, M., Drummond, J. R., Dufour, D., Evans, W. F. J., Fast, H., Fussen, D., Gilbert, K., Jennings, D. E., Llewellyn, E. J., Lowe, R. P., Mahieu, E., McConnell, J. C., McHugh, M., McLeod, S. D., Michaud, R., Midwinter, C., Nassar, R., Nichitiu, F., Nowlan, C., Rinsland, C. P., Rochon, Y. J., Rowlands, N., Semeniuk, K., Simon, P., Skelton, R., Sloan, J. J., Soucy, M.-A., Strong, K., Tremblay, P., Turnbull, D., Walker, K. A., Walkty, I., Wardle, D. A., Wehrle, V., Zander, R., and Zou, J.: Atmospheric Chemistry Experiment (ACE): Mission overview, Geophys. Res. Lett., 32, L15S01, doi:10.1029/2005GL022386, 2005. 16613

Clerbaux, C., Boynard, A., Clarisse, L., George, M., Hadji-Lazaro, J., Herbin, H., Hurtmans, D.,

Title Page

Abstract | Introduction

Conclusions | References

Tables | Figures

|◄ | ►|

◄ | ►

Back | Close

Full Screen / Esc

Printer-friendly Version

Interactive Discussion

Pommier, M., Razavi, A., Turquety, S., Wespes, C., and Coheur, P.-F.: Monitoring of atmospheric composition using the thermal infrared IASI/MetOp sounder, Atmos. Chem. Phys., 9, 6041–6054, doi:10.5194/acp-9-6041-2009, 2009. 16617

Coheur, P.-F., Herbin, H., Clerbaux, C., Hurtmans, D., Wespes, C., Carleer, M., Turquety, S., Rinsland, C. P., Remedios, J., Hauglustaine, D., Boone, C. D., and Bernath, P. F.: ACE-FTS observation of a young biomass burning plume: first reported measurements of C_2H_4, C_3H_6O, H_2CO and PAN by infrared occultation from space, Atmos. Chem. Phys., 7, 5437–5446, doi:10.5194/acp-7-5437-2007, 2007. 16613, 16614

Coheur, P.-F., Clarisse, L., Turquety, S., Hurtmans, D., and Clerbaux, C.: IASI measurements of reactive trace species in biomass burning plumes, Atmos. Chem. Phys., 9, 5655–5667, doi:10.5194/acp-9-5655-2009, 2009. 16614

Crutzen, P. J., Heidt, L. E., Krasnec, J. P., Pollock W. H., and Seiler, W.: Biomass burning as a source of atmospheric gases CO, H_2, N_2O, NO, CH_3Cl, and COS, Nature, 282, 253–256, 1979. 16612

Crutzen, P. J. and Andreae, M. O.: Biomass burning in the tropics: Impact on atmospheric chemistry and biogeochemical cycles, Science, 250, 1669–1678, 1990. 16612

Draxler, R. R. and Rolph, G. D.: HYSPLIT (HYbrid Single-Particle Lagrangian I ntegrated Trajectory) Model, NOAA Air Resources Laboratory, Silver Spring, MD, available at: http://www.arl.noaa.gov/ready/hysplit4.html, 2003. 16616

Fiedler, V., Arnold, F., Ludmann, S., Minikin, A., Hamburger, T., Pirjola, L., Drnbrack, A., and Schlager, H.: African biomass burning plumes over the Atlantic: aircraft based measurements and implications for H2SO4 and HNO3 mediated smoke particle activation, Atmos. Chem. Phys., 11, 3211–3225, doi:10.5194/acp-11-3211-2011, 2011. 16620

George, M., Clerbaux, C., Hurtmans, D., Turquety, S., Coheur, P.-F., Pommier, M., Hadji-Lazaro, J., Edwards, D. P., Worden, H., Luo, M., Rinsland, C., and McMillan, W.: Carbon monoxide distributions from the IASI/METOP mission: evaluation with other space-borne remote sensors, Atmos. Chem. Phys., 9, 8317–8330, doi:10.5194/acp-9-8317-2009, 2009. 16617

Glatthor, N., von Clarmann, T., Stiller, G. P., Funke, B., Koukouli, M. E., Fischer, H., Grabowski, U., Höpfner, M., Kellmann, S., and Linden, A.: Source classification of upper tropospheric pollution by MIPAS HCN and C_2H_6 global distributions, Atmos. Chem. Phys. Discuss., 9, 16197–16232, doi:10.5194/acpd-9-16197-2009, 2009. 16614

Koppmann, R., von Czapiewski, K., and Reid, J. S.: A review of biomass burning emissions, part I: gaseous emissions of carbon monoxide, methane, volatile organic com-

pounds, and nitrogen containing compounds, Atmos. Chem. Phys. Discuss., 5, 10455–10516, doi:10.5194/acpd-5-10455-2005, 2005. 16614

Manney, G. L., Daffer, W. H., Zawodny, J. M., Bernath, P. F., Hoppel, K. W., Walker, K. A., Knosp, B. W., Boone, C., Remsberg, E. E., Santee, M. L., Lynn Harvey, V., Pawson, S., Jackson, D. R., Deaver, L., Pumphrey, H. C., Lambert, A., Schwartz, M. J., Froidevaux, L., McLeod, S., Takacs, L. L., Suárez, M. J., Trepte, C. R., Livesey, N. J., Harwood, R. S., and Waters, J. W.: Solar occultation satellite data and derived meteorological products: sampling issues and comparisons with Aura MLS, J. Geophys. Res., 112, D24S50, doi:10.1029/2007JD008709, 2007. 16616

Li, Q., Jacob, D. J., Yantosca, R. M., Heald, C. L., Singh, H. B., Koike, M., Zhao, Y., Sachse, G. W., and Streets, D. G.: A global three-dimensional model analysis of the atmospheric budgets of HCN and CH_3CN: Constraints from aircraft and ground measurements, J. Geophys. Res., 108(D21), 8827, doi:10.1029/2002JD003075, 2003. 16615

Rinsland, C. P., Dufour, G., Boone, C. D., Bernath, P. F., and Chiou, L.: Atmospheric Chemistry Experiment (ACE) measurements of elevated Southern Hemisphere upper tropospheric CO, C_2H_6, HCN, and C_2H_2 mixing ratios from biomass burning emissions and long-range transport, Geophys. Res. Lett., 32, L20803, doi:10.1029/2005GL024214, 2005. 16614, 16620

Rinsland, C. P., Dufour, G., Boone, C. D., Bernath, P. F., Chiou, L., Coheur, P.-F., Turquety, S., and Clerbaux, C.: Satellite boreal measurements over Alaska and Canada during June–July 2004: Simultaneous measurements of upper tropospheric CO, C_2H_6, HCN, CH_3Cl, CH_4, C_2H_2, CH_3OH, HCOOH, OCS, and SF_6 mixing ratios, Global Biogeochem. Cy., 21, GB3008, doi:10.1029/2006GB002795, 2007. 16614, 16618, 16624, 16633

Simpson, I. J., Akagi, S. K., Barletta, B., Blake, N. J., Choi, Y., Diskin, G. S., Fried, A., Fuelberg, H. E., Meinardi, S., Rowland, F. S., Vay, S. A., Weinheimer, A. J., Wennberg, P. O., Wiebring, P., Wisthaler, A., Yang, M., Yokelson, R. J., and Blake, D. R.: Boreal forest fire emissions in fresh Canadian smoke plumes: C_1-C_{10} volatile organic compounds (VOCs), CO_2, CO, NO_2, NO, HCN and CH_{CN}, Atmos. Chem. Phys. Discuss., 11, 9515–9566, doi:10.5194/acpd-11-9515-2011, 2011.

Singh, H. B., Salas, L., Herlth, D., Kolyer, R., Czech, E., Viezee, W., Li, Q., Jacob, D. J., Blake, D., Sachse, G., Harward, C. N., Fuelberg, H., Kiley, C. M., Zhao, Y., and Kondo, Y.: In situ measurements of HCN and CH_3CN over the Pacific Ocean: Sources, sinks, and budgets, J. Geophys. Res., 108(D20), 8795, doi:10.1029/2002JD003006, 2003. 16615

Torres, O., Chen, Z., Jethva, H., Ahn, C., Freitas, S. R., and Bhartia, P. K.: OMI and MODIS

observations of the anomalous 20082009 Southern Hemisphere biomass burning seasons, Atmos. Chem. Phys., 10, 3505–3513, doi:10.5194/acp-10-3505-2010, 2010. 16614

Tereszchuk, K. A. and Bernath, P. F.: Infrared absorption cross-sections for acetaldehyde (CH_3CHO) in the 3 µm region, J. Quant. Spectrosc. Ra., 112, 990–993, 2011. 16613

Turquety, S., Hurtmans, D., Hadji-Lazaro, J., Coheur, P.-F., Clerbaux, C., Josset, D., and Tsamalis, C.: Tracking the emission and transport of pollution from wildfires using the IASI CO retrievals: analysis of the summer 2007 Greek fires, Atmos. Chem. Phys., 9, 4897–4913, doi:10.5194/acp-9-4897-2009, 2009. 16614

Yokelson, R. J., Susott, R. A., Ward, D. E., Reardon, J., and Griffith, D. W. T.: Emissions from smoldering combustion of biomass measured by open-path Fourier transform infrared spectroscopy, J. Geophys. Res., 102, 18865–18877, 1997. 16614, 16615, 16624

Yokelson, R. J., Bertschi, I. T., Christian, T. J., Hobbs, P. V., Ward, D. E., and Hao, W. M.: Trace gas measurements in nascent, aged, and cloud-processed smoke from African savanna fires by airborne Fourier transform infrared spectroscopy (AFTIR), J. Geophys. Res., 108(D13), 8478, doi:10.1029/2002JD002322, 2003. 16615

Yokelson, R. J., Urbanski, S. P., Atlas, E. L., Toohey, D. W., Alvarado, E. C., Crounse, J. D., Wennberg, P. O., Fisher, M. E., Wold, C. E., Campos, T. L., Adachi, K., Buseck, P. R., and Hao, W. M.: Emissions from forest fires near Mexico City, Atmos. Chem. Phys., 7, 5569–5584, doi:10.5194/acp-7-5569-2007, 2007.

Yokelson, R. J., Karl, T., Artaxo, P., Blake, D. R., Christian, T. J., Griffith, D. W. T., Guenther, A., and Hao, W. M.: The Tropical Forest and Fire Emissions Experiment: overview and airborne fire emission factor measurements, Atmos. Chem. Phys., 7, 5175–5196, doi:10.5194/acp-7-5175-2007, 2007b. 16615

Yokelson, R. J., Crounse, J. D., DeCarlo, P. F., Karl, T., Urbanski, S., Atlas, E., Campos, T., Shinozuka, Y., Kapustin, V., Clarke, A. D., Weinheimer, A., Knapp, D. J., Montzka, D. D., Holloway, J., Weibring, P., Flocke, F., Zheng, W., Toohey, D., Wennberg, P. O., Wiedinmyer, C., Mauldin, L., Fried, A., Richter, D., Walega, J., Jimenez, J. L., Adachi, K., Buseck, P. R., Hall, S. R., and Shetter, R.: Emissions from biomass burning in the Yucatan, Atmos. Chem. Phys., 9, 5785–5812, doi:10.5194/acp-9-5785-2009, 2009.

16620

Table 1. Correlation coefficients (*R*) of tracer-CO calculations made from ACE-FTS measurements of young (2–3 days old) biomass burning plumes originating from a variety of ecosystems. Beneath each R-value (shown in bold) is the slope of the linear regression (i.e. emission ratio) and the standard deviation associated with the regression calculation (shown in parentheses). R-values shown in blue in each ecosystem are those molecules which correlate highly with CO (R-value ≥0.80). Correlations performed on biomass burning emissions can be used effectively to characterize plumes from different ecosystems due to their distinct chemical compositions.

	C_2H_2	C_2H_6	CH_3OH	CH_4	H_2CO	HCN	HCOOH	HNO_3	N_2O_5	NO	NO_2	O_3	OCS
	0.918	**0.939**	**0.937**	**0.115**	**0.702**	**0.932**	**0.885**	**0.149**	**0.815**	**0.296**	**0.971**	**−0.896**	**0.478**
Amazon	0.0014	0.0050	0.0212	0.2311	0.0009	0.0030	0.0024	0.0006	0.0007	0.0004	0.0014	−0.6813	0.0002
	(0.0360)	(0.0711)	(0.2930)	(51.39)	(0.0289)	(0.0374)	(0.0414)	(0.1444)	(0.0467)	(0.0379)	(0.1031)	(30.11)	(0.0204)
	0.962	**0.942**	**0.926**	**0.038**	**0.890**	**0.953**	**0.924**	**−0.301**	**0.896**	**0.251**	**0.201**	**−0.816**	**0.291**
Congo	0.0021	0.0063	0.0192	0.0717	0.0007	0.0052	0.0027	−0.0010	0.0007	0.0002	0.0001	−0.5374	0.0002
	(0.0247)	(0.1037)	(0.3399)	(71.45)	(0.0271)	(0.0942)	(0.0923)	(0.1196)	(0.0794)	(0.0405)	(0.1502)	(27.78)	(0.0161)
	0.951	**0.918**	**0.840**	**0.265**	**0.723**	**0.806**	**0.859**	**−0.872**	**0.867**	**0.591**	**−0.831**	**−0.962**	**0.509**
Savannah	0.0014	0.0048	0.0098	0.2300	0.0012	0.0055	0.0023	−0.0010	0.0015	0.0004	−0.0007	−1.313	0.0001
	(0.0178)	(0.0671)	(0.2895)	(69.19)	(0.0354)	(0.0662)	(0.0816)	(0.0861)	(0.0367)	(0.0094)	(0.0839)	(32.11)	(0.0132)
	0.442	**0.348**	**0.586**	**0.026**	**0.303**	**0.246**	**0.322**	**0.197**	**0.065**	**−0.128**	**0.221**	**−0.326**	**0.046**
Background	0.0009	0.0032	0.0096	0.2413	0.0024	0.0009	0.0049	0.0011	0.0004	−0.0007	0.0027	−0.6948	0.0001
	(0.0170)	(0.1109)	(0.1591)	(88.65)	(0.0285)	(0.0500)	(0.0704)	(0.1218)	(0.0625)	(0.0425)	(0.0967)	(35.79)	(0.0431)
	0.719	**0.931**	**0.846**	**0.095**	**0.832**	**0.613**	**0.928**	**−0.851**	**0.005**	**0.888**	**−0.885**	**−0.909**	**0.019**
Boreal	0.0013	0.0048	0.0217	0.2857	0.0011	0.0015	0.0034	−0.0121	0.0001	0.0012	−0.0003	−2.134	0.0030
	(0.0267)	(0.1065)	(0.6299)	(72.14)	(0.0335)	(0.0354)	(0.1074)	(0.0906)	(0.0307)	(0.0933)	(0.1028)	(34.32)	(0.0331)
	0.594	**0.512**	**0.109**	**0.136**	**0.274**	**0.360**	**0.269**	**−0.231**	**0.052**	**0.209**	**−0.257**	**−0.555**	**0.160**
Background	0.0012	0.0071	0.0347	2.741	0.0015	0.0005	0.0030	−0.0084	0.0002	0.0028	−0.0021	−2.500	0.0002
	(0.0172)	(0.1134)	(0.4629)	(93.24)	(0.0221)	(0.0724)	(0.0429)	(0.3884)	(0.0625)	(0.0498)	(0.1397)	(127.4)	(0.0362)

Table 2. Age comparisons of Canadian Boreal plumes from July 2010 listing the ratios to CO on an excess basis ($\Delta X/\Delta CO$) for plumes 1–2 and 5–6 days old with the associated standard deviation calculations in parenthesis. Calculations were made from approximately 15 measurements of plumes from each representative age. Ratios for the primary pyrogenic species relative to long-lived CO decrease over time as these species are destroyed mainly by reaction with OH as the plume ages, but increased values with negative correlations are noted for O_3, NO_2 and HNO_3 indicating their formation as secondary species.

Trace Species	2–3 Days Old		5–6 Days Old	
	$\Delta X/\Delta CO$	Std. Dev.	$\Delta X/\Delta CO$	Std. Dev.
C_2H_2	0.0015	(0.016)	0.0012	(0.013)
C_2H_6	0.0056	(0.049)	0.0045	(0.029)
CH_3OH	0.037	(0.512)	0.017	(0.446)
CH_4	0.169	(59.37)	0.148	(32.48)
H_2CO	0.0014	(0.0269)	0.0012	(0.0114)
HCN	0.0018	(0.0210)	0.0003	(0.0082)
HCOOH	0.0038	(0.0718)	0.0020	(0.0274)
HNO_3	−0.013	(0.261)	−0.020	(0.163)
NO	0.0006	(0.0167)	0.0012	(0.0227)
NO_2	0.0029	(0.217)	−0.0076	(0.141)
O_3	−2.398	(29.87)	−2.462	(38.85)
OCS	0.0003	(0.0205)	0.0002	(0.0131)

Title Page

Abstract | Introduction

Conclusions | References

Tables | Figures

◀◀ | ▶▶

◀ | ▶

Back | Close

Full Screen / Esc

Printer-friendly Version

Interactive Discussion

Table 3. Tabulated mean concentrations (in ppb) and Tracer-CO correlations for selected trace species from the 5 sequential measurements of the Amazon plume depicted in Fig. 4. Concentrations and R-values for each trace species shown in bold. The associated standard deviation for the calculations are in parenthesis and the emission ratios for the correlations with respect to CO are listed under their respective R-values. Concentrations for the primary pyrogenic species diminish over time while O_3 increases with age. The Tracer-CO correlations confirm these observations including an increasingly large negative correlation for O_3.

	CO	C_2H_2	C_2H_6	CH_3OH	CH_4	H_2CO	HCN	HCOOH	HNO_3	N_2O_5	NO	NO_2	O_3	OCS
Conc.														
sr6532	**139.3**	**0.117**	**0.908**	**1.99**	**1775**	**0.0951**	**0.609**	**0.138**	**0.429**	**0.0796**	**0.0663**	n/a	**89.2**	**0.399**
	(29.12)	(0.024)	(0.139)	(0.491)	(44.03)	(0.039)	(0.0886)	(0.0386)	(0.211)	(0.0472)	(0.0727)		(20.3)	(0.0142)
sr6531	**92.53**	**0.0802**	**0.578**	**0.686**	**1767**	**0.0687**	**0.403**	n/a	**0.291**	**0.0356**	n/a	n/a	**97.6**	**0.418**
	(23.90)	(0.0349)	(0.128)	(0.312)	(31.72)	(0.0463)	(0.0455)		(0.152)	(0.0419)			(30.6)	(0.0161)
sr6530	**98.99**	**0.106**	**0.537**	**1.19**	**1764**	**0.0567**	**0.448**	n/a	n/a	**0.0333**	n/a	n/a	**88.9**	**0.424**
	(34.86)	(0.0543)	(0.170)	(0.746)	(23.66)	(0.0402)	(0.0660)			(0.0230)			(56.0)	(0.0125)
sr6529	**79.13**	**0.0919**	**0.545**	**0.875**	**1733**	**0.0322**	**0.462**	**0.072**	**0.214**	n/a	n/a	**0.284**	**141**	**0.420**
	(28.70)	(0.0664)	(0.179)	(0.651)	(43.49)	(0.0274)	(0.0870)	(0.0774)	(0.061)			(0.082)	(44.1)	(0.0225)
sr6528	**88.19**	**0.0731**	**0.557**	**0.787**	**1767**	**0.0629**	**0.369**	n/a	**0.260**	**0.0502**	**0.0102**	n/a	**96.0**	**0.426**
	(24.48)	(0.0373)	(0.142)	(0.408)	(46.50)	(0.0036)	(0.0970)		(0.076)	(0.0498)	(0.0050)		(28.5)	(0.0119)
Corr.														
	1.000	**0.973**	**0.855**	**0.802**	**−0.384**	**0.441**	**0.913**	**0.409**	**0.128**	**0.628**	**−0.059**		**−0.192**	**0.700**
sr6532	1.000	0.0009	0.0041	0.0135	−0.5807	0.0006	0.0031	0.0005	0.0009	0.0011	−0.0001	n/a	−0.1339	0.0004
	(0.000)	(0.0061)	(0.0767)	(0.3111)	(43.12)	(0.0373)	(0.0387)	(0.0472)	(0.2220)	(0.0397)	(0.0784)		(21.10)	(0.0108)
	1.000	**0.949**	**0.975**	**0.885**	**0.536**	**0.627**	**0.975**		**0.726**	**0.738**			**−0.880**	**0.899**
sr6531	1.000	0.0014	0.0051	0.0119	0.7117	0.0012	0.0033	n/a	0.0048	0.0012	n/a	n/a	−1.127	0.0006
	(0.000)	(0.0117)	(0.0298)	(0.1530)	(28.08)	(0.0379)	(0.0110)		(0.1030)	(0.0305)			(15.28)	(0.0075)
	1.000	**0.981**	**0.960**	**0.933**	**0.077**	**0.614**	**0.894**			**0.862**			**−0.935**	**0.692**
sr6530	1.000	0.0014	0.0044	0.0199	0.0523	0.0007	0.0029	n/a	n/a	0.0005	n/a	n/a	−1.503	0.0002
	(0.000)	(0.0112)	(0.0513)	(0.2842)	(25.02)	(0.0337)	(0.0331)			(0.0128)			(21.03)	(0.0097)
	1.000	**0.977**	**0.979**	**0.994**	**−0.640**	**0.998**	**0.997**	**0.969**	**−0.620**			**0.984**	**−0.671**	**0.697**
sr6529	1.000	0.0022	0.0061	0.0225	−0.9699	0.0010	0.0045	0.0026	−0.0013	n/a	n/a	0.0028	−1.033	0.0005
	(0.000)	(0.0167)	(0.0443)	(0.0868)	(0.8232)	(0.0022)	(0.0001)	(0.0235)	(0.0585)			(0.0176)	(40.11)	(0.0198)
	1.000	**0.785**	**0.983**	**0.906**	**0.290**	**0.891**	**0.996**		**0.287**	**0.887**	**0.496**		**−0.845**	**0.653**
sr6528	1.000	0.0011	0.0053	0.0144	0.5511	0.0013	0.0047	n/a	0.0009	0.0018	0.0001	n/a	−0.9832	0.0003
	(0.000)	(0.0247)	(0.0280)	(0.1834)	(46.90)	(0.0174)	(0.0025)		(0.0769)	(0.0248)	(0.0047)		(16.03)	(0.0097)

Table 4. ACE Emission factors relative to CO compared to emission factors calculated from airborne measurements (Akagi et al., 2010) of Boreal forests in Canada, the Amazon Rainforest and the savannah of northern Australia. Previously calculated Boreal emission factors made by Rinsland et al. (2007) using ACE-FTS measurements of young Boreal fires in Canada are also included in the comparison.

| Trace Species	Canada Boreal Forest			Amazon Rainforest		Australia Savannah	
	EF (g kg^{-1})	EF$_{Rinsland}$ (g kg^{-1})	EF$_{Akagi}$ (g kg^{-1})	EF (g kg^{-1})	EF$_{Akagi}$ (g kg^{-1})	EF (g kg^{-1})	EF$_{Akagi}$ (g kg^{-1})
C_2H_6	0.656 ± 0.964	0.906 ± 0.195	1.79 ± 1.14	0.49 ± 0.02	0.68 ± 0.28	0.304 ± 0.017	0.31 ± 0.20
CH_3OH	3.13 ± 0.516	2.73 ± 0.707	2.82 ± 1.61	2.23 ± 0.09	2.31 ± 0.88	0.663 ± 0.082	0.77 ± 0.23
HCN	0.159 ± 0.036	0.201 ± 0.057	1.52 ± 0.81	0.265 ± 0.031	0.42 ± 0.26	0.312 ± 0.031	0.35 ± 0.092
HCOOH	0.706 ± 0.119	0.654 ± 0.161	0.57 ± 0.46	0.367 ± 0.033	0.27 ± 0.23	0.224 ± 0.033	0.81 ± 0.071
OCS	0.027 ± 0.059	0.053 ± 0.018	0.46 ± 0.47	0.039 ± 0.007	0.025	0.013 ± 0.008	n/a
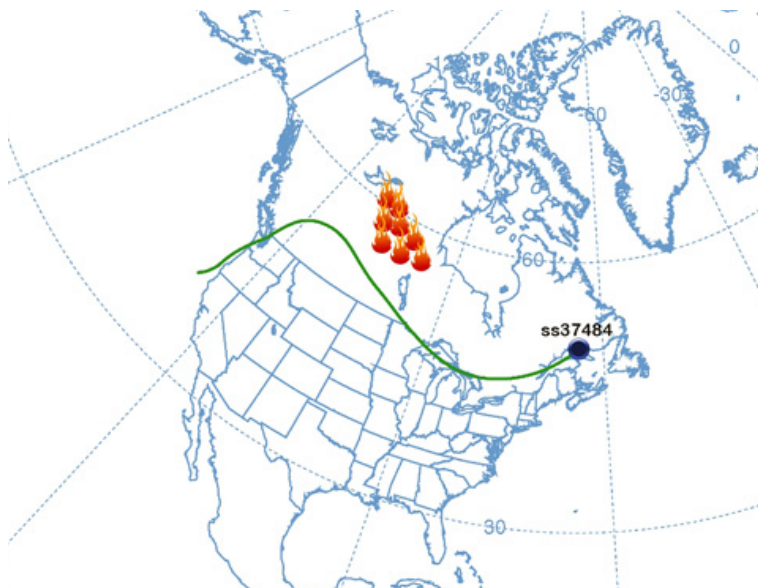
Fig. 1. A sample output of the trajectory data obtained using HYSPLIT. The 3-day back trajectory calculated from occultation ss37484 measured on 29 July 2010 displayed with the location of instances of Boreal fires burning in northern Saskatchewan and parts of the Northwest Territories in Canada on 26 July 2010. Spatial and temporal coincidence of the trajectories confirm the measurement source location.
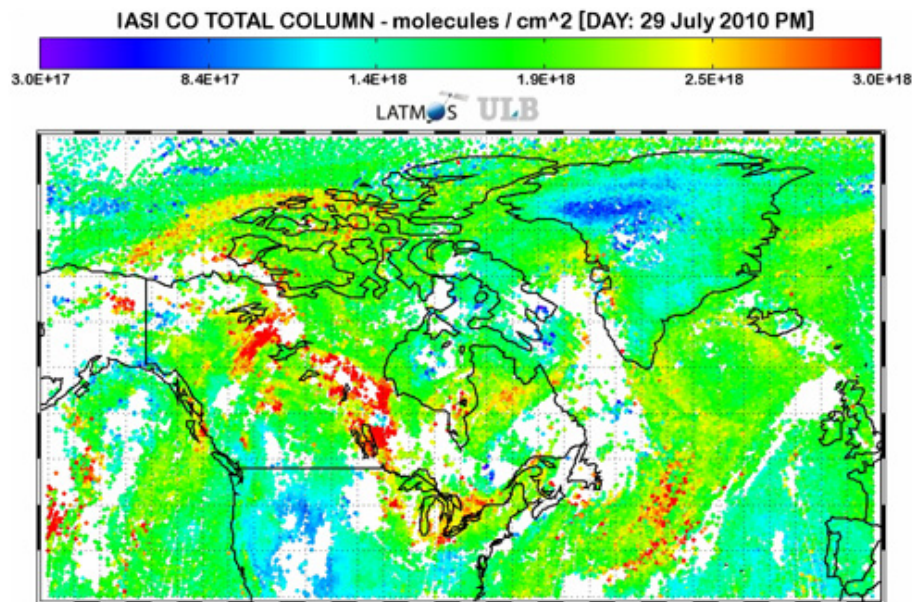
Fig. 2. IASI CO total column data for the evening orbit over North America on 29 July 2010. The figure shows the biomass burning outflow from numerous sources including Boreal fires in northern Saskatchewan and the Northwest Territories in Canada, a Siberian plume making its way eastward over Arctic Canada and a plume originating from China off the west coast of North America. The plume of elevated CO sampled by ss37484 is clearly visible over Maritime Canada.
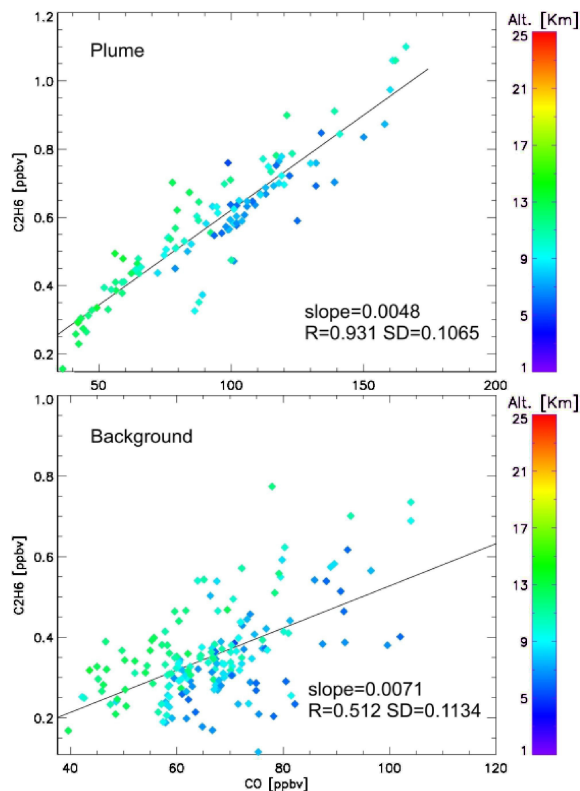
Fig. 3. C_2H_6-CO correlations for ACE-FTS measurements made in July 2008. (Upper panel) Correlations of approximately 30 measurements made of Boreal biomass burning plumes in Canada (2–3 days old). The high positive (R) coefficient for C_2H_6 indicates its presence in the plume as a primary pyrogenic species. (Lower panel) Correlations of an equivalent number of off-plume, background measurements made during the same time period at similar latitudes.
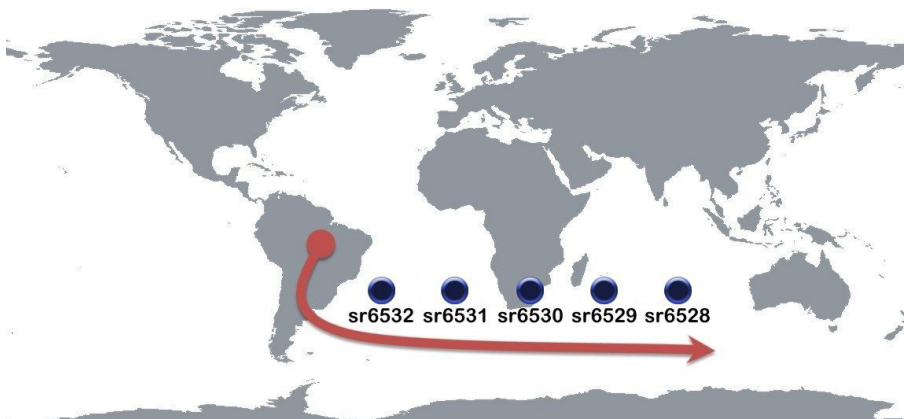
Fig. 4. Example of sequential ACE-FTS measurements sampling a continuous plume outflow originating from the Amazon on 20 October 2004.

Title Page

Abstract | Introduction

Conclusions | References

Tables | Figures

◄ | ►

Back | Close

Full Screen / Esc

Printer-friendly Version

Interactive Discussion